Reflection mode photoacoustic measurement of speed of sound

Roy G. M. Kolkman[1], Wiendelt Steenbergen[1], and Ton G. van Leeuwen[1,2]

[1]University of Twente, Faculty of Science & Technology, Biophysical Engineering, PO Box 217, NL-7500 AE Enschede, the Netherlands
[2] University of Amsterdam, Academic Medical Center, Laser Center PO Box 22700, NL-1100 DE Amsterdam, the Netherlands
r.g.m.kolkman@utwente.nl

Abstract: We present a method to determine the speed of sound in tissue using a double-ring photoacoustic sensor working in reflection mode. This method uses the cross-correlation between the laser-induced ultrasound waves detected by two concentric ring shaped sensors, while a priori information about the depth-position of the photoacoustic source is not required. We demonstrate the concept by estimating the speed of sound in water as a function of temperature. Comparison of the estimated speed with values reported in literature shows an average systematic error of 0.1% and a standard deviation of 0.1%. Furthermore, we demonstrate that the method can be applied to layered media. The method has application in the correction of photoacoustic and ultrasound images afflicted by local speed variations in tissue. Additionally, the concept shows promise in monitoring temperature changes which are reflected in speed of sound changes in tissue.

OCIS Codes: (170.5120) Photoacoustic imaging; (170.0110) Imaging systems; (170.4580) Optical diagnostics for medicine; (300.1030) Absorption.

References and links:

1. H.F. Zhang, K. Maslov, G. Stoica, L.V. Wang, "Functional photoacoustic microscopy for high-resolution and noninvasive in vivo imaging," Nat. Biotechnol. **24**, 848-851 (2006).
2. R.A. Kruger, W.L. Kiser, D.R. Reinecke, G.A. Kruger, "Thermoacoustic computed tomography using a conventional linear transducer array," Med. Phys. **30,** 856-860 (2003).
3. R.G.M. Kolkman, E. Hondebrink, W. Steenbergen, F.F.M. de Mul, "In vivo photoacoustic imaging of blood vessels using an extreme-narrow aperture sensor," IEEE J Sel Top Quantum Electron **9**, 343-346 (2003).
4. R.G.M. Kolkman, N. Bosschaart, B. Kok, T.G. van Leeuwen, W. Steenbergen, "Photoacoustic imaging of valves in superficial veins," Lasers Surg. Med. **38**, 740-744 (2006)
5. J.J. Niederhauser, M. Jaeger, R. Lemor R, P. Weber, and M. Frenz, "Combined ultrasound and optoacoustic system for real-time high-contrast vascular imaging in vivo," IEEE Trans. Med. Imaging 24 (4), 436-440 (2005).
6. R.I. Siphanto, K.K. Thumma, R.G.M. Kolkman, T.G. van Leeuwen, F.F.M. de Mul, J.W. van Neck, L.N.A. van Adrichem, W. Steenbergen, "Serial noninvasive photoacoustic imaging of neovascularization in tumor angiogenesis," Opt. Express **13**, 89-95 (2005).
7. J.C. Bamber, "Acoustical characteristics of biological media," in Encyclopedia of Acoustics, M.J. Crocker Ed., (J. Wiley & Sons, New York, 1997), pp. 1703-1726.
8. R.G.M. Kolkman, E. Hondebrink, W. Steenbergen, T.G. van Leeuwen, "Photoacoustic imaging with a double-ring sensor featuring a narrow aperture," J. Biomed. Optics **9**, 1327-1335 (2004)
9. R.G.M. Kolkman, J.H.G.M. Klaessens, E. Hondebrink, J.C.W. Hopman, F.F.M. de Mul, W. Steenbergen, J.M. Thijssen, T.G. van Leeuwen, "Photoacoustic determination of blood vessel diameter," Phys. Med. Biol. **49**, 4745-4756 (2004)
10. C.G.A. Hoelen, F.F.M. de Mul, "A new theoretical approach to photoacoustic signal generation," J Acoust. Soc. Am. **106**, 695-706 (1999).
11. J. Lubbers, and R. Graaff, "A simple and accurate formula for the sound velocity in water," Ultrasound Med. Biol. **24**, 1065 (1998).

#77319 - $15.00 USD Received 21 November 2006; revised 12 January 2007; accepted 12 January 2007

12. J. Ophir, and T. Lin, "A calibration-free method for measurement of sound speed in biological tissue samples," IEEE Trans. Ultrason. Ferroelectr. Freq. Control **35**, 573 (1988).
13. M.E. Anderson, and G.E. Trahey, "The direct estimation of sound speed using pulse-echo ultrasound," J. Acoust. Soc. Am. **104**, 3099 (1998).
14. Z. Yuan, Q. Zhang, H. Jiang, "Simultaneous reconstruction of acoutic and optical properties of heterogeneous media by quantitative photoacoustic tomography," Opt. Express **14**, 6749-6754 (2006).

1. Introduction

Photoacoustic (PA) imaging is a hybrid imaging technique that uses pulsed light to induce ultrasound. This ultrasound arises due to thermoelastic expansion at positions where pulsed light is absorbed. PA imaging therefore can be applied to study optical absorbing structures in tissue, such as blood vessels.[1-6] To reconstruct PA images from the detected ultrasound waves, knowledge is needed about the speed of sound in the tissue, which is often assumed to be about 1540 m/s. However, the speed of sound for soft tissue ranges from 1350 m/s for fat to 1700 m/s for skin.[7] Another complication is the inhomogeneous composition of tissue which makes the assumption of a constant speed of sound invalid. These issues can lead to serious image artifacts in ultrasound or photoacoustic image reconstruction. Consequently a method to determine the speed of sound in tissue is highly desirable. Additionally, knowledge of the speed of sound can be used to identify various tissue types. In this paper a simple and accurate method is presented to determine the speed of sound from the measured PA time traces using a PA sensor consisting of two concentric annular piezoelectric elements[3]. Results are shown from speed of sound measurements of water as a function of temperature as well as measurements of the speed of sound in layered media.

2. Materials & methods

2.1 Photoacoustic system

To detect laser-induced pressure transients, a home-built double-ring photoacoustic sensor [3] was employed. In short, this double-ring sensor consisted of 2 concentric ring-shaped sensor surfaces with equal areas (diameter: inner ring 4 x 4.34 mm; outer ring 7 x 7.2 mm). The pressure transients were detected by 25 μm thick PVdF (Piezotech SA, France), biaxially stretched, electrically polarized, with one side Au/Pt metallized, which was glued to the electrodes. The photoacoustic signals were amplified by amplifiers with a high pass cut off frequency at about 1 MHz. This sensor had an angular aperture of 1.5 – 10 degrees (-6 dB of directivity pattern) for acoustic signals with a peak-to-peak time of 67 ns – 350 ns, respectively. The time traces detected by this sensor were digitized by a dual channel oscilloscope (TDS210, 250 Msample/sec, 60 MHz bandwidth, Tektronix) and the acquisition was synchronized on the detection of the laser-pulse by a photodiode.

2.2 Estimation of the speed of sound

Ultrasound signals originating from a PA source located at the midline of the sensor arrive at the two ring-shaped sensors at different times as shown in Fig. 1, and therefore have to be corrected for their mutual time delay. By applying this time delay, the time t_i' at which the signals are detected by the rings is corrected such that the corrected time t corresponds to the depth z_0 ($t = z_0/c_0$) of the PA source: $t = \{[(c_0\ t_i')^2 - R_i^2]^{1/2}\}/c_0$, where R_i is the radius to the center of the inner (*in*) or outer (*out*) ring-shaped detection area and c_0 the speed of sound. This procedure, which is comparable to dynamic focusing in ultrasound imaging, requires knowledge of c_0. Assumption of a speed of sound c deviating from the real speed of sound c_0 will lead to not exactly coinciding PA signals $P(t)$ of both rings. A measure for the coincidence of the signals is the cross-correlation $C(\Delta t) \equiv \int P_{in}(t)P_{out}(t+\Delta t)dt$ between the two signals. $C(\Delta t)$ will be maximum for the time delay Δt that is needed to make the signals of the inner and outer ring exactly coincident. When the PA source is located on the central axis of the double-ring sensor, the value of $C(\Delta t=0)$ is dependent on the assumed speed c, and consequently can be used to precisely determine the speed of sound c_0 of the medium. $C_0(c) \equiv$

#77319 - $15.00 USD Received 21 November 2006; revised 12 January 2007; accepted 12 January 2007

$C(\Delta t=0, c)$ will be maximum for an assumed speed c equal to the real speed of sound c_0 in the tissue.

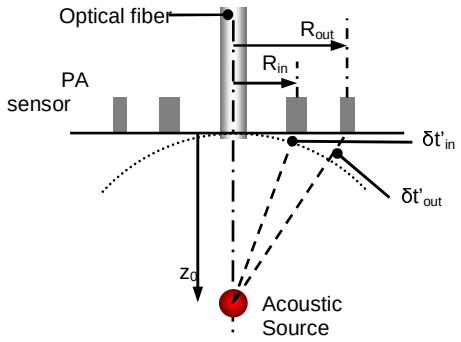

Fig. 1. Time-delays $\delta t'_{in}$ and $\delta t'_{out}$ when using a double-ring PA sensor to detect acoustic waves from a source located at depth z_0.

First an analytical expression for $C_0(c)$ will be derived for a PA source located on the midline of the ring-shaped sensor. The double-ring sensor has an extreme narrow aperture, which implies that signals originating from locations off-axis do not contribute significantly to the detected signal. In our previous work [8,9] we have shown that because of this narrow aperture we could approximate cylindrical sources (like blood vessels) reasonably well with the model of a spherical PA source. Therefore we assume a spherical PA source located on the midline of the ring-shaped sensor, at a depth z_0 inside a medium with a speed of sound equal to c_0. At a distance $\mathbf{r}$ from the PA source, the pressure transient generated by a laser pulse (Gaussian temporal profile) can be described by[10]

$$P(\mathbf{r},t) = -P_{\max}(\mathbf{r})\sqrt{e}\,\frac{t-\tau}{\frac{1}{2}\tau_{pp}}\exp\left[-\frac{1}{2}\left(\frac{t-\tau}{\frac{1}{2}\tau_{pp}}\right)^2\right], \tag{1}$$

with $\tau = r/c_0$, and τ_{pp} the peak to peak time (time difference between the occurrence of the positive and negative peak). This acoustic wave is detected by the i^{th} ring-shaped sensor at a time $t_i'=\tau_i$. From this time t_i', the depth z_i is calculated by assuming a speed of sound c:

$$z_i = \sqrt{(ct_i')^2 - R_i^2} = \sqrt{\left(\frac{c}{c_0}\right)^2\left(z_0^2 + R_i^2\right) - R_i^2}\,, \tag{2}$$

with $i = in, out$. The depth z_i will only be equal to the real depth z_0 if the assumed speed of sound c is equal to the actual speed c_0. Based on this depth z_i now an expression can be derived for the laser-induced pressure wave $P_i(z_i,t)$ corrected for the time-delay, i.e. the acoustic wave in the center of the ring shaped sensor surface, by taking $\tau_i = z_i/c$. Using $P_i(z_i,t)$, the cross-correlation at $\Delta t=0$ as a function of speed of sound $C_0(c)$ can be calculated:

$$C_0(c) \propto \frac{\sqrt{\pi}}{2\tau_{pp}}\left[2-\left(\frac{\tau_{in}(c)-\tau_{out}(c)}{\frac{1}{2}\tau_{pp}}\right)^2\right]\exp\left[-\frac{1}{4}\left(\frac{\tau_{in}(c)-\tau_{out}(c)}{\frac{1}{2}\tau_{pp}}\right)^2\right], \tag{3}$$

#77319 - $15.00 USD Received 21 November 2006; revised 12 January 2007; accepted 12 January 2007

$$\tau_i(c) = \frac{\sqrt{\frac{c^2}{c_0^2}\left(z_0^2 + R_i^2\right) - R_i^2}}{c}. \quad (4)$$

When a second order Taylor series expansion of $\tau_i(c)$ around c_0 is made and is substituted in equation 3 one can write:

$$C_0(c) \propto \frac{\sqrt{\pi}}{2\tau_{pp}}\left[2 - \left(\frac{c-c_0}{c_0^2}\right)^2\left(A - \frac{c-c_0}{c_0}B\right)^2\right] \exp\left[-\tfrac{1}{4}\left(\frac{c-c_0}{c_0^2}\right)^2\left(A - \frac{c-c_0}{c_0}B\right)^2\right] \quad (5)$$

with $A = 2(R_{in}^2 - R_{out}^2)/(z_0\tau_{pp})$, and $B = A\,[3/2 + (R_{in}^2 + R_{out}^2)/(2z_0^2)]$ This expression can be fitted to the measured $C_0(c)$ curves to yield c_0, without prior knowledge about τ_{pp} or z_0. In Fig. 2 the calculated $C_0(c)$ curves are shown for a spherical PA source with a peak-to-peak time of 40 ns, located at three different depths in a medium with c_0= 1540 m/s, for R_{in} = 2.085 mm, and R_{out} = 3.55 mm. As expected, the maximum of these curves occurs at c_0. With increasing depth, the cross-correlation curve broadens. This broadening is caused by the difference in time delay between the inner and outer ring that decreases with increasing depth.

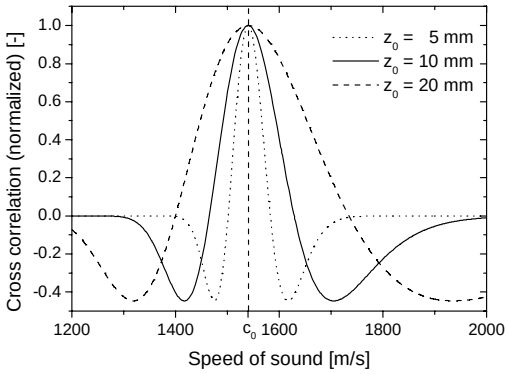

Fig. 2. Calculated $C_0(c)$ curves for various depth locations z_0 of PA source, assuming c_0=1540 m/s and τ_{pp}= 40 ns.

The proposed method can be applied to determine the effective speed of sound c_0 of the tissue between the acoustic source (located at depth z_0) and the sensor. In case of layered media (N layers, layer i: speed of sound c_i, thickness d_i), this effective speed of sound consists of contributions of all these layers (Fig. 3):

$$\frac{1}{c_0} = \frac{1}{z_0}\sum_{i=1}^{N}\frac{d_i}{c_i}. \quad (6)$$

The thickness d_i can be estimated from the depth z_i that follows from multiplying $\tau(c_i)$ by the estimated speed of sound c_i.

The velocity in each layer can be determined when in each layer an acoustic source is present. In photoacoustic imaging, the main acoustic source (optical absorber) in tissue is blood. This implies that well-localized sources, in the form of blood vessels, are present throughout the tissue. By scanning the sensor over the tissue surface, these blood vessels can be localized. Thus, for each of these vessels the effective speed of sound in the tissue above these vessels can be estimated. Subsequently, the speed of sound distribution can be reconstructed using equation 6.

#77319 - $15.00 USD Received 21 November 2006; revised 12 January 2007; accepted 12 January 2007

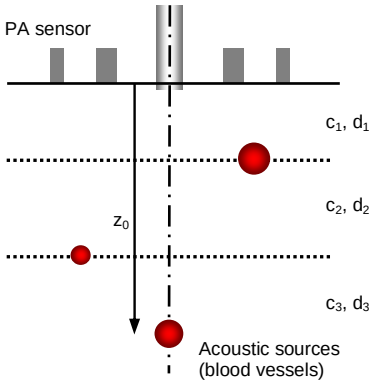

Fig. 3. Schematic overview of layered tissue, consisting of three layers with thickness d_i, and speed of sound c_i.

2.3 Speed of sound in water as a function of temperature

To demonstrate our method, the speed of sound in water as a function of temperature was determined. Demineralised water was degassed by boiling it for about 10 minutes. The water was left to cool down to room temperature before the measurement was started. During the measurement the temperature of the water was slowly increased to above 40˚C, by heating the reservoir by a laboratory heating plate. The temperature of the water was monitored with a thermocouple.

As a model for an optically absorbing structure in tissue (e.g. blood vessel) we used a 200 μm diameter black horsetail hair. The hair was illuminated through a 100 μm diameter fiber, placed at about 1 mm from the hair, by light from an OPO (wavelength 710 nm, 10 ns pulse-duration, repetition rate 10 Hz), pumped by an Nd:YAG laser (Brilliant B, Quantel + OPO, Opotek Inc.). This hair acted as a PA source, located at a depth of about 10 mm with respect to the sensor, generating a bipolar PA signal with a peak-to-peak time of 40 ns. First the hair was localized by making a B-scan. Next, the sensor was positioned exactly above the hair and the PA time traces, detected by the inner and outer rings of our PA sensor were measured and were averaged 64 times.

2.4 Speed of sound in layered media

To validate the applicability of our method to layered media, measurements were performed on a sheet of Perspex (d=1.89mm, measured with a caliper) and a sheet of silicone rubber (d=0.96mm). Photoacoustic sources were created by drawing a line with a black pencil at the top and bottom of these sheets. The sheets were immersed in demineralised water to create a two-layer model: a layer of water with a thickness of about 7.5 mm and a layer of Perspex or silicone rubber (Fig. 4).

#77319 - $15.00 USD Received 21 November 2006; revised 12 January 2007; accepted 12 January 2007

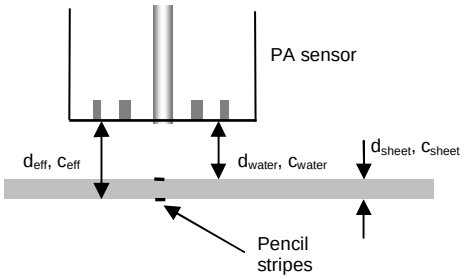

Fig. 4. Schematic overview of the layered phantom, consisting of two layers: a layer of water with thickness d_{water}, and speed of sound c_{water}, and a sheet of rubber or Perspex with thickness d_{sheet}, and speed of sound c_{sheet}.

Photoacoustic signals were generated by illuminating the pencil stripes through the optical fiber which was integrated inside the PA sensor, by light from an OPO+Nd:YAG laser-system (wavelength 800 nm, 10 ns pulse-duration, repetition rate 20 Hz, Opolette, Opotek Inc.). The pencil-stripes were localized by making a B-scan, consisting of 101 measurement positions with a spacing of 100 µm. The PA time traces, detected by the inner and outer rings of our PA sensor were averaged 16 times.

The proposed method was applied to signals detected at a position exactly above the stripes. When applying the method to the photoacoustic signals generated by the pencil stripe at the top of the sheet, the method will yield the speed of sound of water c_{water}. Applying the method to the lower pencil stripe will yield an effective speed of sound c_{eff}, which is a combination of the speed of sound in water and the speed of sound in the sheet. Next, the speed of sound in the sheet material was calculated by applying equation (6). The thicknesses d_{water} and d_{eff} were calculated by multiplying the arrival time of the photoacoustic pressure transients τ_{water} and τ_{eff} by the estimated speed of sound c_{water} and c_{eff} respectively.

Besides estimation of the speed of sound in the perspex and silicone rubber sheet from the photoacoustic pressure transients, the speed of sound was also estimated using pulse-echo ultrasound. This was done by replacing the photoacoustic sensor by a 15 MHz focused ultrasound transducer (V319-SU, Panametrics) which emitted a 15 Mhz burst. From the time delay Δt between the echo from the upper and lower part of the sheet the speed of sound was estimated: $c_{sheet} = 2d_{sheet}/\Delta t$, while d_{sheet} was estimated with a caliper.

3. Results

3.1 Speed of sound in water as a function of temperature

The cross-correlation of the measured signals of the inner and outer ring was calculated as a function of speed of sound. In Fig. 5 the resulting curve is shown for a temperature of 26.4˚C. The actual speed of sound in water was determined by fitting equation 5 to the obtained cross-correlation curve. (Fig. 5, dashed line).

#77319 - $15.00 USD Received 21 November 2006; revised 12 January 2007; accepted 12 January 2007

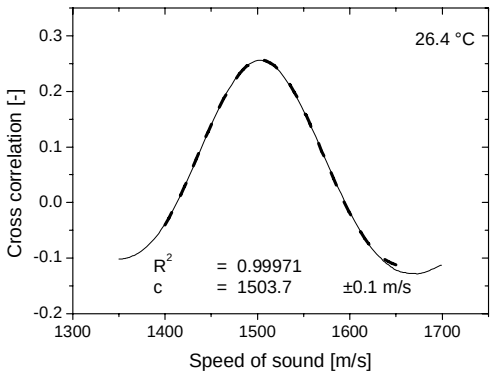

Fig. 5. $C_0(c)$ curve of the speed of sound in water at 26.4 ˚C. The actual speed of sound is determined by fitting equation 5 to the $C_0(c)$ curve as depicted by the dashed line.

The speed of sound as a function of the measured temperature range at atmospheric pressure is shown in Fig. 6, together with values reported in literature.[11]

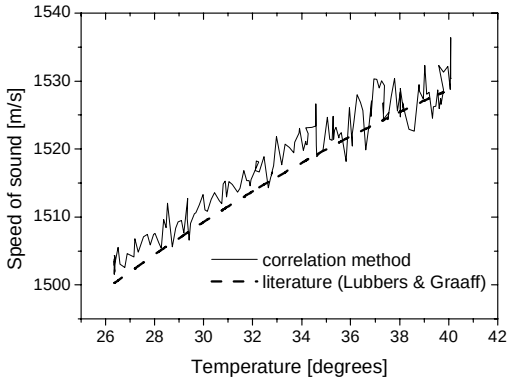

Fig. 6. Speed of sound, as determined with our correlation method, as a function of temperature. The model of Lubbers & Graaff [11] (using their coefficients C2) is plotted for comparison (dashed line).

3.2 Speed of sound in layered media

The cross-correlation curves for the photoacoustic signals from the pencil stripes at the upper and lower part of the sheet were calculated for the sheet of rubber [Fig.7(a)] and Perspex [Fig.7(b)].

#77319 - $15.00 USD Received 21 November 2006; revised 12 January 2007; accepted 12 January 2007

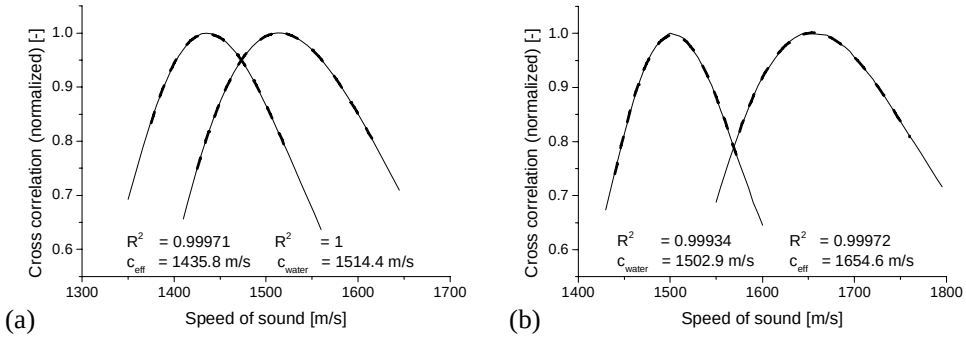

Fig. 7. $C_0(c)$ curves of the water-rubber layered system (a) and the water-perspex layered system (b). The speed of sound of water c_{water} and the effective speed of sound c_{eff} are determined by fitting equation 5 to the $C_0(c)$ curve as depicted by the dashed lines.

The speed of sound in the layer of rubber and layer of Perspex was calculated from the estimated c_{water} and c_{eff} by using equation 6. The resulting values for the speed of sound and thickness of these layers are shown in table 1. In this table also the values for the speed of sound are listed which were obtained from the pulse-echo method. For interpretation of the results of the pulse-echo method, the thickness of the layers was estimated with a caliper.

Table 1. Speed of sound and thickness of a layer of Perspex and Silicone rubber as estimated with the PA cross-correlation method compared with values obtained from pulse-echo ultrasound measurements and thickness measured with a caliper.

	Pulse-echo method		*PA Cross-correlation*	
	Thickness *d* [mm]	Speed of sound *c* [m/s]	Thickness *d* [mm]	Speed of sound *c* [m/s]
Perspex	1.89 ± 0.05	2700 ± 91	1.86 ± 0.02	2754 ± 34
Silicone rubber	0.96 ± 0.05	1005 ± 34	0.94 ± 0.02	1002 ± 12

4. Discussion

In this paper the use of a method to estimate the speed of sound using a double-ring photoacoustic sensor was demonstrated. This method uses the cross-correlation between the laser-induced ultrasound waves detected by two concentric ring shaped sensors, while a priori information about the depth-position of the photoacoustic source is not required.

4.1 Homogeneous media

Estimation of the speed of sound in water showed that the correlation of the model with the measured $C_0(c)$ curves was high ($R^2 > 0.999$), and the standard error in the estimated speed of sound was less than 0.01% (Fig. 5). Comparison of our measured speed of sound in water as a function of temperature with values reported in literature showed an average systematic error of 0.1%. (Fig. 6). The standard deviation of the estimated speed was 0.1%. The accuracy in the temperature measurement was not taken into account, but a deviation in temperature of ±0.5ºC will lead to an error in the estimated speed of sound of ±0.1%.

It has to be noted that the finite width of the ring-shaped detection area causes a broadening of the photoacoustic signals. However, this broadening of the signals is nearly

#77319 - $15.00 USD Received 21 November 2006; revised 12 January 2007; accepted 12 January 2007

equivalent for both inner and outer ring for sources located at a depth larger than 4 mm. As this will be valid for all practical cases, the broadening does not affect our calculations.

An alternative method that can achieve an accuracy comparable to our method is the ultrasound transmission method of Ophir and Lin[12]. They could achieve an error in the estimated speed of sound of 0.1%. However, this method can only be applied to cases where both sides of the tissue can be accessed. A direct method to estimate the speed of sound using pulse-echo ultrasound from the one-way delay profile has been reported by Anderson and Trahey.[13] They were able to estimate the speed of sound with an error less than 0.4%, and under the most ideal experimental conditions an error of 0.1%, which is comparable to the results we obtained. However, the speed of sound estimations at a single temperature (standard error 0.01%) indicate that our method has the potential to obtain an accuracy better than 0.1%.

4.2 Layered media

It has been shown that the speed of sound in a layered system can be estimated without prior knowledge about the thickness of the layer or distance between the layer and the sensor. The error in the estimated speed of sound in the layered system increased to 1% due to an addition of errors because of application of equation (6).

The values for the speed of sound in Perspex and silicone rubber were in agreement with values obtained with pulse-echo ultrasound (table 1). However, the pulse-echo ultrasound method required prior knowledge of the layer thickness and therefore this thickness had to be measured with a caliper.

The observed differences in the estimated speed of sound of the water during the measurement of the layered systems (Fig. 7) can be explained by a difference in temperature of the water which was about 27 ºC in case of the measurement on Perspex and 30 ºC in case of the measurement on the rubber layer.

In the proposed method we did not take into account the effect of refraction of acoustic waves. For a more accurate estimation of the speed of sound it will be advantageous to incorporate this refraction in our calculations. Nevertheless, the obtained results were in good agreement with the results obtained with pulse-echo ultrasound.

Recently Yuan et.al.[14] presented an iterative method to simultaneously reconstruct acoustic and optical properties in photoacoustic tomography. For their experiments they used a circular scanning geometry which requires full access to all sides of the object. However, our method can be operated in reflection, requiring access to only one side of the object.

4.3 Applications

The proposed method can be applied in ultrasound as well as photoacoustic imaging provided that clear acoustic sources can be identified. In ultrasound imaging, acoustic sources are formed by reflection at positions with acoustic impedance mismatches in tissue. This mainly occurs at the edges of different tissue structures. In photoacoustic imaging, the main acoustic source (optical absorber) in tissue is blood. This implies that since well localized sources, in the form of blood vessels, are present throughout the tissue, photoacoustic imaging has the potential to estimate speed of sound distributions *in vivo*.

These speed of sound distributions can be used to improve the quality of photoacoustic or ultrasound images by using these distributions to reconstruct the image. At this moment, often an average value for the speed of sound in tissue of 1540 m/s is assumed throughout the whole imaged volume. This can result in serious deformation artifacts in the reconstructed image, especially in high-resolution imaging. As our method can in principle be applied to any detection geometry, it has a potential application in high-resolution photoacoustic as well as ultrasound imaging equipment to improve image quality.

In Fig. 8 the effect is shown of the assumed speed of sound on the reconstruction [3] of a photoacoustic image of a 200 µm diameter black hair immersed in water. Photoacoustic signals were generated by illuminating the hair with pulsed light at a wavelength of 690 nm (Brilliant B + OPO, Quantel SA, France) and pulse duration of 10 ns. A B-scan was

#77319 - $15.00 USD Received 21 November 2006; revised 12 January 2007; accepted 12 January 2007

performed consisting of 101 A-scans with a spacing of 20 µm. Applying our method to the detected signals yielded a speed of sound of 1492 m/s (image A). In image B and C a speed of sound was assumed which was deviating from the actual value. As a result the contrast in the images B and C decreased to respectively 94% and 82% of the contrast that is observed in image A. Furthermore, the -6dB lateral/axial resolution increased from 359/146 µm in image A to 384/155 µm in image C. In addition the depth at which the image of the hair is observed increased with 0.35 mm for image C.

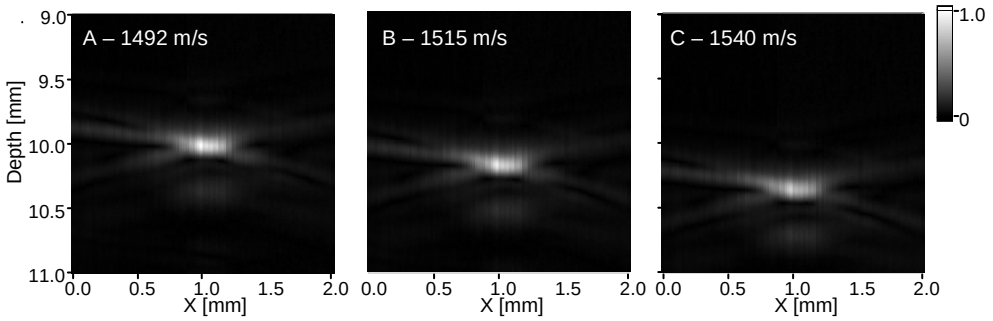

Fig. 8. Photoacoustic images of a 200 µm diameter black hair immersed in water. Images are reconstructed as a function of speed of sound A – 1492 m/s (equal to the actual speed of sound), B – 1515 m/s, and C – 1540 m/s.

For soft tissue the speed of sound ranges from 1350 m/s for fat to 1700 m/s for skin.[7] Hence, knowledge of the local speed of sound will enable identification of tissue-types, which eventually can be applied to discriminate between healthy and diseased tissue. In addition, the speed of sound is dependent on the temperature. As a result, measurement of speed of sound can reveal information about local tissue temperature. This might have applications in monitoring temperature during thermal therapy of tissue.

5. Conclusion

In conclusion, we have developed a method that can be used to determine the effective speed of sound in the tissue volume between the PA source (blood vessel) and the double ring PA detector. In addition we have shown that this method can be applied to layered media. This method has promising applications in correction of PA images for speed of sound inhomogeneities and in identification of various tissue types by their speed of sound. Furthermore, the method can be used to monitor temperature-induced changes in speed of sound inside tissue. This method is not limited to PA imaging, but can also be applied in pulse-echo ultrasound imaging using any detection geometry with at least two sensor elements at different distances to the acoustic source.

Acknowledgments

This work was supported by the Netherlands Foundation of Fundamental Research on Matter FOM (grant 00PMT22) and the Institute for BioMedical Technology (BMTI) of the University of Twente.

#77319 - $15.00 USD Received 21 November 2006; revised 12 January 2007; accepted 12 January 2007